SCIENTIA AGROPECUARIA

Scientia Agropecuaria

Web page: http://revistas.unitru.edu.pe/index.php/scientiaagrop

Facultad de Ciencias Agropecuarias

Universidad Nacional de Trujillo

RESEARCH ARTICLE

A validated ordinal diagrammatic severity scale for zucchini yellow mosaic virus in *Cucurbita moschata*: Screening for tolerant accessions in Peru

Fiorella Gonzales-Borda[1, 2]; Dustin Marin-Gil[1]; Isabel Montes-Yarasca[2]; Alexis Dueñas-Dávila[2]; Alejandro Risco-Mendoza[1*]

[1] Department of Plant Pathology, Agronomy Faculty, Universidad Nacional Agraria La Molina, Lima, Perú.
[2] Department of Horticulture, Agronomy Faculty, Vegetable Crop Group, Universidad Nacional Agraria La Molina, Lima, Perú.

* Corresponding author: alejandrorisco@lamolina.edu.pe (A. Risco-Mendoza).

Received: 25 April 2026. Accepted: 12 October 2026. Published: 22 October 2026.

Abstract

The squash (*Cucurbita moschata*), a landrace crop with a denomination of origin in Lambayeque, Peru, represents a valuable genetic resource with potential for tolerance or resistance to potyviruses. Among these, zucchini yellow mosaic virus (ZYMV) is one of the most destructive viral pathogens affecting cucurbits worldwide. This study aimed to develop and validate a diagrammatic ordinal scale for assessing ZYMV disease severity under field conditions and to identify resistant accessions. In 2024, sixteen accessions were evaluated under natural infection in an experimental field of the Vegetable Research Program at the Universidad Nacional Agraria La Molina, Peru. Following previous virus confirmation via RT-PCR and HTS sequencing, disease monitoring included symptom characterization and virus detection by DAS-ELISA, which confirmed a high incidence of ZYMV. Utilizing a dataset of 40 leaf samples representing different severity levels, a four-level ordinal diagrammatic scale was developed by integrating visual foliar symptomatology with relative viral concentration (optical density) obtained from DAS-ELISA. The scale was validated through field evaluations using independent raters, and its reliability was assessed using Fleiss' kappa and Cohen's kappa statistics. The proposed scale demonstrated high biological accuracy, revealing a strong, highly significant correlation between visual severity levels and serological viral concentration (Spearman's $\rho = 0.937$, $p < 0.0001$). Inter-rater reliability assessments confirmed strong overall reproducibility among independent evaluators (Fleiss' kappa = 0.608, $p < 0.001$). Statistical analysis revealed a highly significant differential response among genotypes; accession C44 exhibited the lowest and most stable severity levels, closely followed by C09, establishing them as highly promising sources of resistance. This study provides a reliable tool for ZYMV severity assessment and supports the identification of genetic resources for resistance breeding programs in cucurbits. The scale developed in this study will help standardize symptom assessment and improve the identification and selection of resistant plant materials, thereby enhancing the efficiency of resistance breeding programs.

Keywords: aligned rank transform; DAS-ELISA; kappa test; phytopathometry; plant disease epidemiology; potyvirus; resistance breeding; tropical pumpkin.

DOI: https://doi.org/10.17268/sci.agropecu.2026.062

Cite this article:

Gonzales-Borda, F., Marin-Gil, D., Montes-Yarasca, I., Dueñas-Dávila, A., & Risco-Mendoza, A. (2026). A validated ordinal diagrammatic severity scale for zucchini yellow mosaic virus in *Cucurbita moschata*: Screening for tolerant accessions in Peru. *Scientia Agropecuaria*, *17*(4), 943-961.

1. Introduction

The Peruvian "squash" (*Cucurbita moschata* Duchesne) has significant historical and cultural relevance in Peru. Currently, this species is cultivated in sixteen regions of the country and is recognized for its high gastronomic value and its denomination of origin in Lambayeque (Arbizu et al., 2022; Saldaña Serrano et al., 2024). However, cucurbits are affected by various viruses, among which potyviruses are particularly prominent (Ghoshal et al., 2026; Silva et al., 2019; Simmons et al., 2011). The zucchini yellow mosaic virus (ZYMV; species: *Potyvirus cucurbitaflavitesselati*) is one of the most destructive pathogens of cucurbits worldwide, capable of reducing yields by up to 94% (Blua and Perring, 1989; Kheder et al., 2017; Chen et al., 2026). This virus has flexuous particles and a single-stranded positive-sense RNA genome [ssRNA (+)]. It is transmitted by aphids in a non-persistent manner and, in susceptible plants, induces foliar mosaic, stunted growth, and severe fruit malformations, along with discoloration that renders fruits unmarketable (Shafie et al., 2026; Abdel Aleem et al., 2021; Simmons et al., 2011). In Peru, its presence was recently detected in *Cucurbita maxima* during the 2022 and 2023

cropping seasons (Valencia et al., 2025), its occurrence has also been confirmed in zucchini (*Cucurbita pepo*) and squash (*Cucurbita moschata*) (Riquelme-Verastegui et al., 2026).

Management of potyviruses relies primarily on the use of genetically resistant cultivars, which is considered the most effective strategy (Fidan et al., 2023; Li et al., 2024; Hao et al., 2024), as tolerant genetic material allows productivity to be maintained despite infection. However, its use remains controversial due to the risk of latent infections and viral spread (Moura et al., 2005). In the Peruvian context, a critical scientific gap exists, evidenced by the lack of breeding programs focused on developing *C. moschata* cultivars with resistance or tolerance that can be incorporated into improvement programs. This is compounded by the absence of standardized tools for assessing viral severity, as well as robust scales that enable effective selection of materials with resistance or tolerance potential, whether monogenic or polygenic (Dhillon et al., 2021; Schafleitner et al., 2024). Nevertheless, effective genes against ZYMV have been identified in *Cucurbita* spp. (Paris et al., 1988; Gilbert-Albertini et al., 1993; Pachner et al., 2011; Brown et al., 2003), particularly in *C. moschata*, where resistance is mainly governed by dominant genes (Brown et al., 2003; Shrestha et al., 2021; Li et al., 2024); however, their incorporation into commercial varieties remains limited (Lecoq & Desbiez, 2008).

Severity, traditionally defined as the proportion of the evaluated unit area exhibiting disease symptoms (Nutter et al., 1991), is a widely used variable in the assessment of plant diseases caused by phytopathogens. However, in the case of plant viruses such as ZYMV, its estimation is challenging because symptom expression follows a different pattern and does not show a direct relationship with the affected area (Xu et al., 2004; Bock et al., 2022). In such cases, severity is mainly expressed through qualitative traits, such as mosaic intensity, morphological distortions, and other phenotypic alterations.

The level of severity of viral diseases is influenced by multiple factors, including virus identity, plant age at the time of infection, and environmental conditions, among others (Díaz et al., 2010; de la Iglesia & Elena, 2023). Assessment using specific scales allows damage to be quantified and constitutes a key tool for cultivar selection in breeding programs (Candian et al., 2021; Caligiore-Gei et al., 2022; Schafleitner et al., 2024). In this context, the development of accurate, precise and reproducible severity scales is essential for decision-making in both field conditions and breeding programs. Furthermore, these evaluation tools must meet statistical assumptions; when ordinal values are derived from qualitative data, nonparametric methods are required for scale validation (Shah & Madden, 2004; Madden et al., 2007a; Wobbrock et al., 2011).

Given the recent detection of ZYMV in Peru (Valencia et al., 2025) and the risk it poses to cucurbit production systems, this study aims to develop and validate an ordinal diagrammatic scale to assess the severity of ZYMV-induced virosis in *C. moschata* under field conditions at UNALM, as well as to determine the tolerance levels of sixteen accessions evaluated during the 2024 cropping season.

2. Methodology

2.1. Study Site

This study was conducted at the (i) Research and Social Outreach Program in Vegetables, as well as (ii) the Virology Laboratory, greenhouse, and mesh house of the Academic Department of Plant Pathology, Faculty of Agronomy, Universidad Nacional Agraria La Molina, located in the district of La Molina, Lima Region, Peru, at 12°04'54" S latitude, 76°56'33" W longitude, and an altitude of 239 m above sea level.

2.2. Plant Material

A total of sixteen *C. moschata* accessions were evaluated, each represented by an individual fruit harvested during the 2022 growing season. Fruits were selected according to their distinctive phenotypic characteristics (Table 1 and Figure 1).

2.3. Field establishment of *C. moschata* accessions

Between July 2024 and February 2025, the field experiment was conducted. Therefore, the seeds from each *C. moschata* accession were germinated in Petri dishes containing paper towels moistened with sterile distilled water and incubated at a constant temperature of 28 °C for four days. For this procedure, sixteen seeds were used per accession, and those showing vigorous germination were subsequently selected.

Germinated seeds, with radicles approximately 2 mm in length and hook-shaped apices, were transplanted into 72-cell seedling trays previously disinfected with a 1% sodium hypochlorite solution. A pre-moistened commercial substrate (Rekyva) was used. The trays were kept inside an aphid-proof mesh structure for nine days, until the seedlings reached the stage of the first pair of true leaves.

During this 9-day period, seedlings were evaluated by direct visual observation for symptoms

associated with viral infection. Individuals showing suspicious symptoms were transferred to the Phytovirology Greenhouse, where viral infection was confirmed by mechanical inoculation onto indicator plants susceptible to potyviruses (*C. pepo* cv. 'Gray Zucchini').

Seedlings were transplanted to a 2,516 m² experimental field on July 9, 2024, after pre-transplant irrigation had been applied through a drip irrigation system 24 h before transplanting. A spacing of 3 m between plants and 2 m between twin rows was used.

2.4. Experimental design

The sixteen accessions were established under field conditions using a Simple Lattice Design with two replicates (Figure A1). Replicates were used to provide repeated evaluation of each accession under the field conditions and to account for spatial variability within the experimental area. Each accession was considered a treatment and was represented by four plants in each experimental unit; they were used to provide multiple plants for field evaluation while maintaining the planned experimental area. In total 128 plants were distributed over an area of 2,516 m². Treatments were randomly assigned within the experiment, in each replicate of the lattice arrangement, using the *agricolae* package of the R software implemented in RStudio (version 4.3.3).

2.5. Viral symptom characterization and virus identification

Symptom characterization was based on records of previous potyvirus infections in *C. pepo* and *C. moschata* (Riquelme-Verastegui et al., 2026). Symptoms included mosaic on leaves and fruits, protuberances and blister-like lesions on both organs, as well as leaf distortion and reduced leaf area. Evaluations for symptoms associated with viral infection began in the first week after crop establishment. Symptoms were recorded in a field data sheet including accession identification and symptom type.

In the same experimental area, during 2022 and 2023, the Virology and Vegetable Program team identified the potyvirus ZYMV using High-Throughput Sequencing (HTS), reverse transcription polymerase chain reaction (RT-PCR), and Double Antibody Sandwich Enzyme-Linked Immunosorbent Assay (DAS-ELISA) (Valencia et al., 2025). Based on this background, virus detection in the experimental field was performed by DAS-ELISA using ZYMV-specific antibodies (QC-SOP-0087 Anl. 002, Version 2.0; DSMZ, Braunschweig, Germany), according to the manufacturer's instructions. Plants previously inoculated with the ZYMV_Lim isolate (Valencia et al., 2025) and maintained in an insect-proof screenhouse were used as positive controls, whereas healthy *C. moschata* plants maintained separately under the same conditions served as negative controls. Mechanical inoculations were also carried out in *C. pepo* cv. 'Gray Zucchini' for biological confirmation of the pathogen.

2.6. Detection and confirmation of viral infection in field-grown accessions

To confirm viral infection in plants from the sixteen accessions established in the field, leaf tissue was collected from plants showing symptoms associated with viral infection at two time points, 90 and 104 days after transplanting (dat). The samples were transported to the "César Fribourg Solís" Phytovirology Laboratory at UNALM for DAS-ELISA analysis. The ZYMV_Lim (GenBank: OQ181225.1) inoculum (Valencia et al., 2025) was used as the positive control, whereas a healthy *C. moschata* plant served as the negative control.

Table 1

Phenotypic characteristics of sixteen *C. moschata* accessions correspond to the accession code from the germplasm bank of the Vegetable Research Program, "El Huerto", UNALM

No.	Accession code	Fruit description	No. of plants per replicate A + B
1	C08	Yellow/orange parental	4 + 4
2	C09	Yellow/orange parental	4 + 4
3	C10	Green parental	4 + 4
4	C25	Yellow/orange parental	4 + 4
5	C32	Orange (primary) with green spots (secondary)	4 + 4
6	C36	Orange (primary) with green spots (secondary)	4 + 4
7	C39	Yellow/orange parental	4 + 4
8	C41	Chimera	4 + 4
9	C42	Chimera	4 + 4
10	C44	Green parental	4 + 4
11	C50	Green (primary) with orange spots (secondary)	4 + 4
12	C51	Chimera	4 + 4
13	C57	Green (primary) with orange spots (secondary)	4 + 4
14	C59	Green parental	4 + 4
15	C67	Green parental	4 + 4
16	C68	Green (primary) with orange spots (secondary)	4 + 4

2.7. Mechanical transmission assay

The mechanical transmission assay was conducted to verify the presence of the virus in plants exhibiting atypical symptoms not necessarily associated with viral infections, as well as in those showing typical symptomatology. For this purpose, leaves with visible symptoms were collected on two occasions, at 155 and 172 dat, and were macerated in a mortar with 2 mL of distilled water until an extract was obtained. Mechanical inoculation was performed on cotyledonary leaves of *C. pepo* cv. 'Gray Zucchini', previously dusted with carborundum abrasive (600 mesh), by manually applying the extract. Three replicates were conducted for each case, including their respective mock controls, which were inoculated with distilled water only. Subsequently, the plants were maintained in an aphid-proof mesh house under controlled conditions.

2.8. Development of a disease severity scale

Leaf sampling and DAS-ELISA detection of ZYMV

At 217 dat, a total of 40 leaf samples were randomly collected, each from a different plant, representing a range of symptom severity from asymptomatic to severely symptomatic plants. Samples were transported in polystyrene containers with ice and stored in plastic bags to avoid direct handling and subsequently maintained at 4 °C until processing. Each sample was individually coded and documented through photographic records.

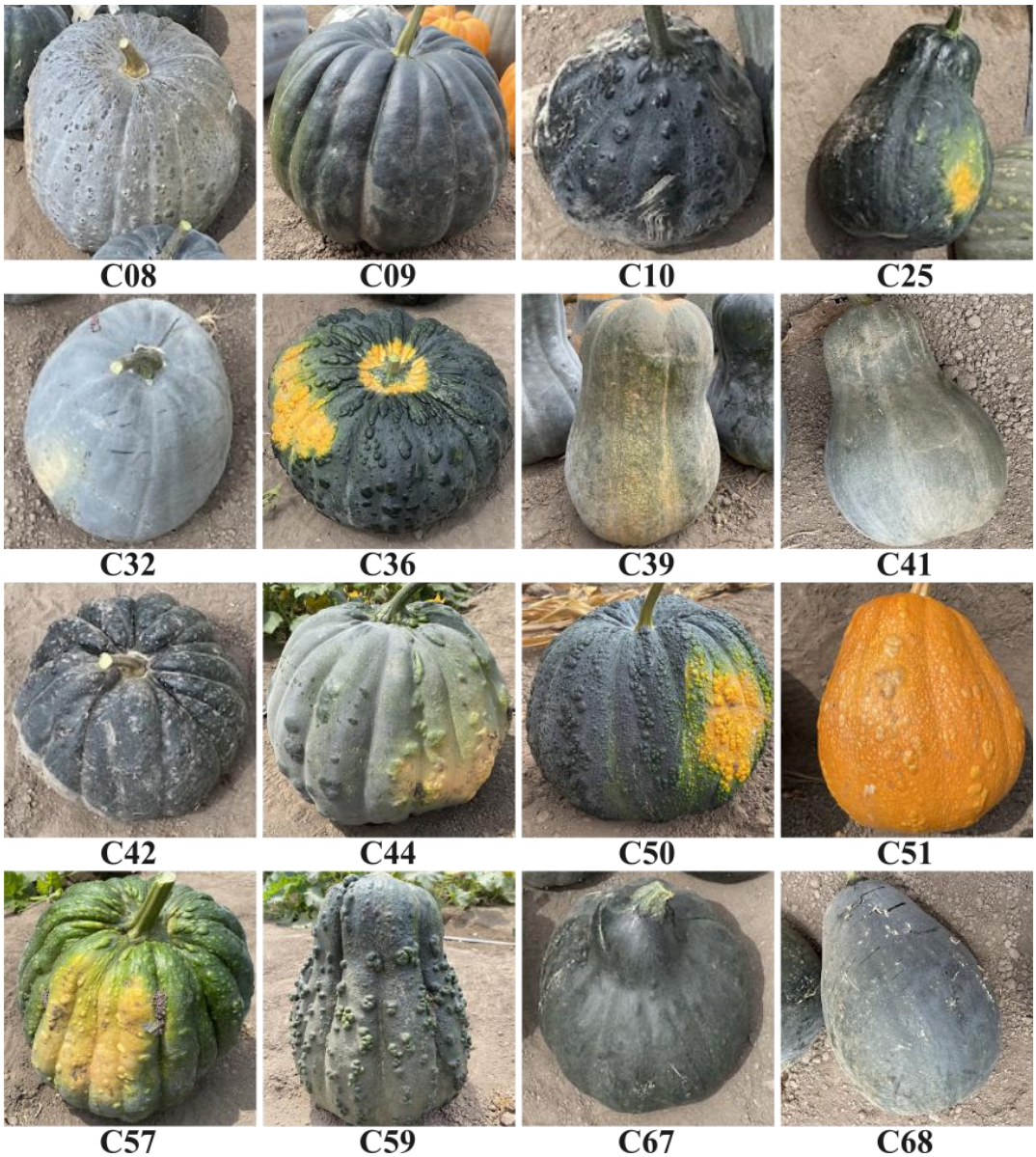


Figure 1. Fruits of the sixteen *C. moschata* accessions. The numbers shown at the bottom of each image correspond to the accession code from the germplasm bank of the Vegetable Research Program, "El Huerto", UNALM.

For analysis, 0.05 g of leaf tissue was weighed and macerated in an extraction buffer at a 1:20 (w/v) ratio. Samples were evaluated by DAS-ELISA using specific antibodies against ZYMV (QC-SOP-0087; DSMZ, https://www.dsmz.de/) following the manufacturer's instructions. ELISA plates were read at an absorbance of 405 nm using a BioTek EPOCH spectrophotometer, and data were processed using Gen5 software. Samples were considered positive when absorbance values were equal to or greater than three times the mean of the negative control.

Diagrammatic severity scale

For the development of the severity scale (Figure 2), two criteria were considered: (i) the similarity of symptomatology observed in photographic records and (ii) comparable optical density values obtained through DAS-ELISA. Based on these groupings, a qualitative ordinal diagrammatic scale was developed to represent different levels of disease severity.

2.9. Validation and field application of the ZYMV severity scale

Biological consistency of the severity scale levels

To validate the biological accuracy of the proposed ordinal visual scale, the relationship between assigned severity levels and virus antigen concentration was evaluated via DAS-ELISA. Given that severity was recorded as an ordinal variable (levels 1 – 4) and serological absorbance (OD at 405 nm) is a continuous quantitative variable that does not necessarily follow a normal distribution, Spearman's Rank Correlation Coefficient (ρ) was employed (Turechek, 2004; Navasca et al., 2025). This analysis allowed quantifying the intensity and direction of the monotonic association between the visual scale and the viral load, without assuming a linear relationship between ranks. Statistical processing was performed with the *stats* package of the software R (version 4.3.3).

Application of the severity scale to compare ZYMV severity among accessions

For field validation of the scale, four raters (E1, E2, E3, and E4), who underwent a standardized training session in the recognition of ZYMV symptoms in *C. moschata*, participated in the field assessment at 224 dat, when 100% disease incidence was recorded. The training included a detailed explanation of the assessment criteria and symptom characteristics using a reference set of images representing each severity level. To familiarize the raters with the symptom thresholds, the images were presented in ascending order of severity for 30 seconds each. From each of the sixteen accessions and two replicates, three leaves (H1, H2, and H3) were randomly chosen for evaluation. Each rater independently assessed the same leaves *in situ* by direct visual inspection, with a maximum assessment time of 30 seconds per leaf, using the diagrammatic scale: asymptomatic (level 1), low (level 2), intermediate (level 3), and high severity (level 4). Data were recorded following the order: accession, rater, leaf, and severity level.

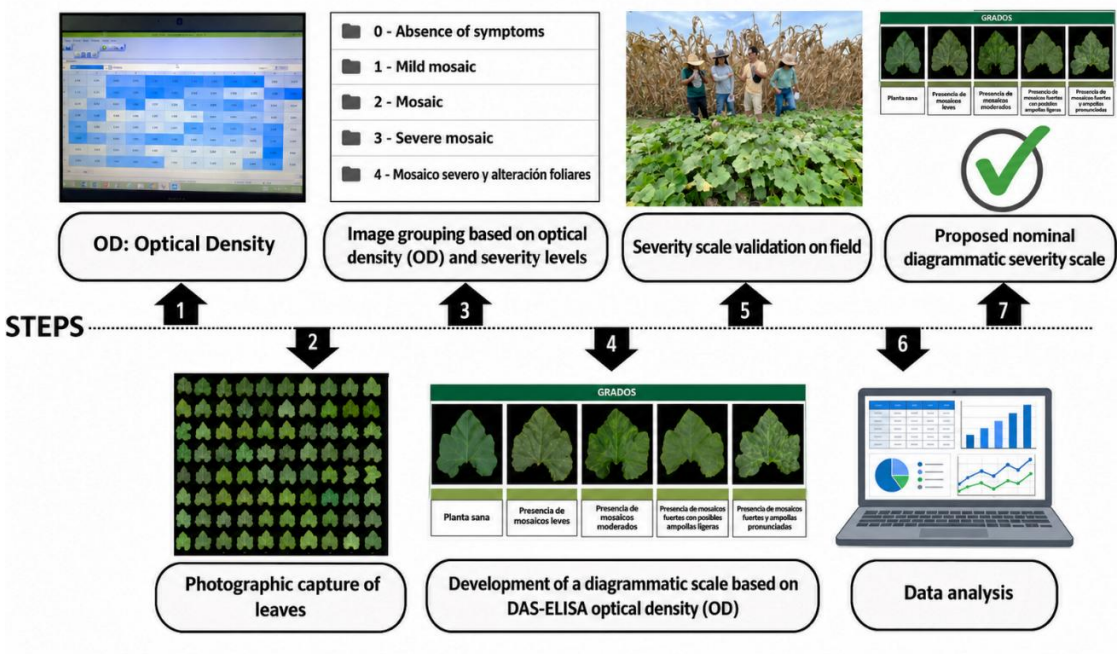


Figure 2. Stages in the development of diagrammatic disease severity scale.

Evaluation of inter-rater agreement across severity levels

Overall agreement among the four evaluators across all severity levels was assessed for the 96 evaluated leaves (16 accessions × 3 leaves × 2 replicates) using the concordance Fleiss' kappa test (α = 0.05), while pairwise agreement between evaluators was determined using concordance Cohen's kappa test (α = 0.05) (Madden et al. 2007b). Additionally, agreement at each severity level of the scale was evaluated across all corresponding observations using Fleiss' kappa test (α = 0.05). All analyses were performed using the *irr* package in R software, version 4.3.3.

Comparison of severity levels among *C. moschata* genotypes using the severity scale

Even though the spatial arrangement was initially mapped following a Simple Lattice design with two replicates, the statistical analysis was performed treating these main replicates as complete randomized units to accommodate the non-parametric nature of the response variable. ZYMV severity was compared among accessions using values obtained from a proposed four-level ordinal scale. Due to the ordinal nature of the data and the replicated experimental design, the nonparametric Aligned Rank Transform (ART) method was applied (Shah & Madden, 2004; Wobbrock et al., 2011). This approach isolates factor effects through a mathematical alignment prior to rank assignment, enabling the use of analysis of variance (ANOVA) (Madden et al., 2007a). The unit of observation was the individual leaf. To robustly capture intra-plot variability and control visual assessment error, an intensive sub-sampling strategy was applied, evaluating twelve observational leaves per experimental plot (incorporating independent sample ratings by four evaluators). This hierarchical sub-sampling quantified the within-plot variance required to computationally test the statistical significance (α = 0.05) of the effects of accession, replicate, and the accession x replicate interaction using an ANOVA based on the aligned ranks and the F-test. To identify accessions with lower severity, estimated marginal means were calculated from the aligned rank linear model, and multiple pairwise comparisons were performed using t-tests with Bonferroni correction (α = 0.05). All analyses were conducted in R software (v. 4.3.3), using the *ARTool* and *emmeans* packages.

Additionally, the statistical dependence between accessions and ZYMV severity levels was assessed using the chi-square (χ^2) test of independence at a 5% significance level (α = 0.05). Due to expected frequencies below five, significance was estimated through Monte Carlo simulations with 2,000 replicates. Specific associations were identified using standardized Pearson residuals, considering values greater than 1.96 or less than −1.96 as significant. Additionally, effect size was quantified using Cramér's V coefficient. These analyses were conducted in R software (v. 4.3.3), using the *chisq.test* function of the stat package and the *rcompanion* package.

3. Results and discussion

3.1. Symptom development in *C. moschata* and ZYMV detection

During the initial evaluations, conducted between weeks one and eighteen after transplanting from August to November 2024, nonspecific foliar symptoms were observed. These included mild chlorosis, leaf deformation, generalized chlorosis of the leaf blade, and irregularly distributed chlorotic areas on both the surface and margins of the leaves (Figure 3). Initially, these symptoms were considered indicative of possible viral infections. However, DAS-ELISA analysis yielded negative results for ZYMV, indicating that the symptoms described in Figure 4 were not associated with infection by this virus but rather corresponded to nonspecific manifestations. This observation was further confirmed through mechanical inoculation assays using indicator plants, in which no development of symptoms associated with viral infection was observed (Figure 3, upper section). Collectively, these findings confirm that the symptoms observed during the first eighteen weeks were not caused by viral agents.

However, during a second evaluation conducted between weeks nineteen and 26 after transplanting, from December 2024 to January 2025, the appearance of more specific symptoms consistent with viral infections was observed, including chlorotic mottling, mosaic patterns, and leaf blistering (Figure 3, lower section). These findings were also confirmed by DAS-ELISA, allowing a more precise detection of the causal agent.

Variation in disease severity is likely influenced by multiple factors, including genotype, plant developmental stage, and environmental conditions (Gea-Caballero & Aranda, 2026; Ahsan et al., 2023), which in turn can negatively affect leaf growth and pigment content (Mahmoud et al., 2025). Symptom expression in *Cucurbita* spp. is highly variable, ranging from yellow mosaic, leaf deformation, severe blistering, and knobbed fruits (Ali et al., 2024) to the complete absence of visible symptoms in resistant cultivars (Shrestha et al., 2021).

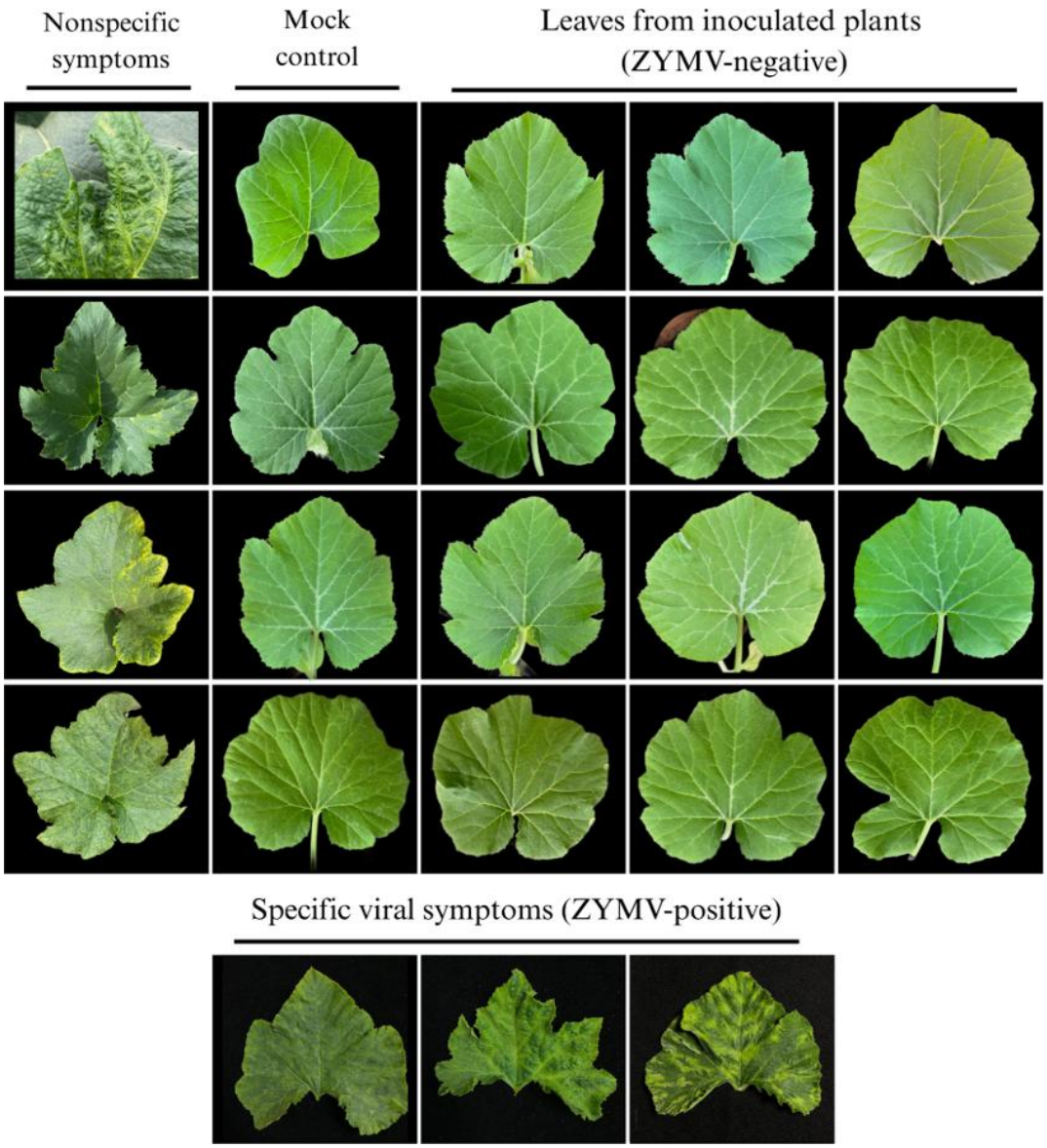


Figure 3. Nonspecific symptoms in *C. moschata* and ZYMV-associated symptomatology. The upper section illustrates five symptom types observed during the first 18 weeks after transplanting, which were not associated with ZYMV, as confirmed by mechanical inoculation assays in *C. pepo* cv. 'Gray Zucchini'. The lower section shows three representative symptoms associated with ZYMV infection from week sixteen onward, confirmed by DAS-ELISA.

3.2. Serological analysis and threshold determination for ZYMV

Randomly selected leaf samples analyzed by DAS-ELISA using ZYMV-specific antibodies showed a range of optical density values. A threshold value of 0.64 was established, with samples exhibiting values equal to or greater than this cutoff considered positive (Figure A2).

Absorbance in ELISA assays is commonly measured at 405 nm; however, the cut-off value used to discriminate between positive and negative samples is not universal, as it depends on the methodological approach and the objective of the analysis. In this study, the interpretation of results was based on previously reported criteria. On the one hand, samples with absorbance values at least twice those of healthy plants have been considered positive (Ali et al., 2024). On the other hand, a more stringent criterion defines positivity when the optical density (OD) is equal to or greater than the mean of the negative controls plus three times the standard deviation (Boissinot et al., 2017), thereby reducing the likelihood of false positives. Likewise, in plant breeding programs aimed at selecting pathogen-resistant genotypes, a conservative threshold of three times the mean OD of the negative control has also been applied (Ibiza et al., 2010).

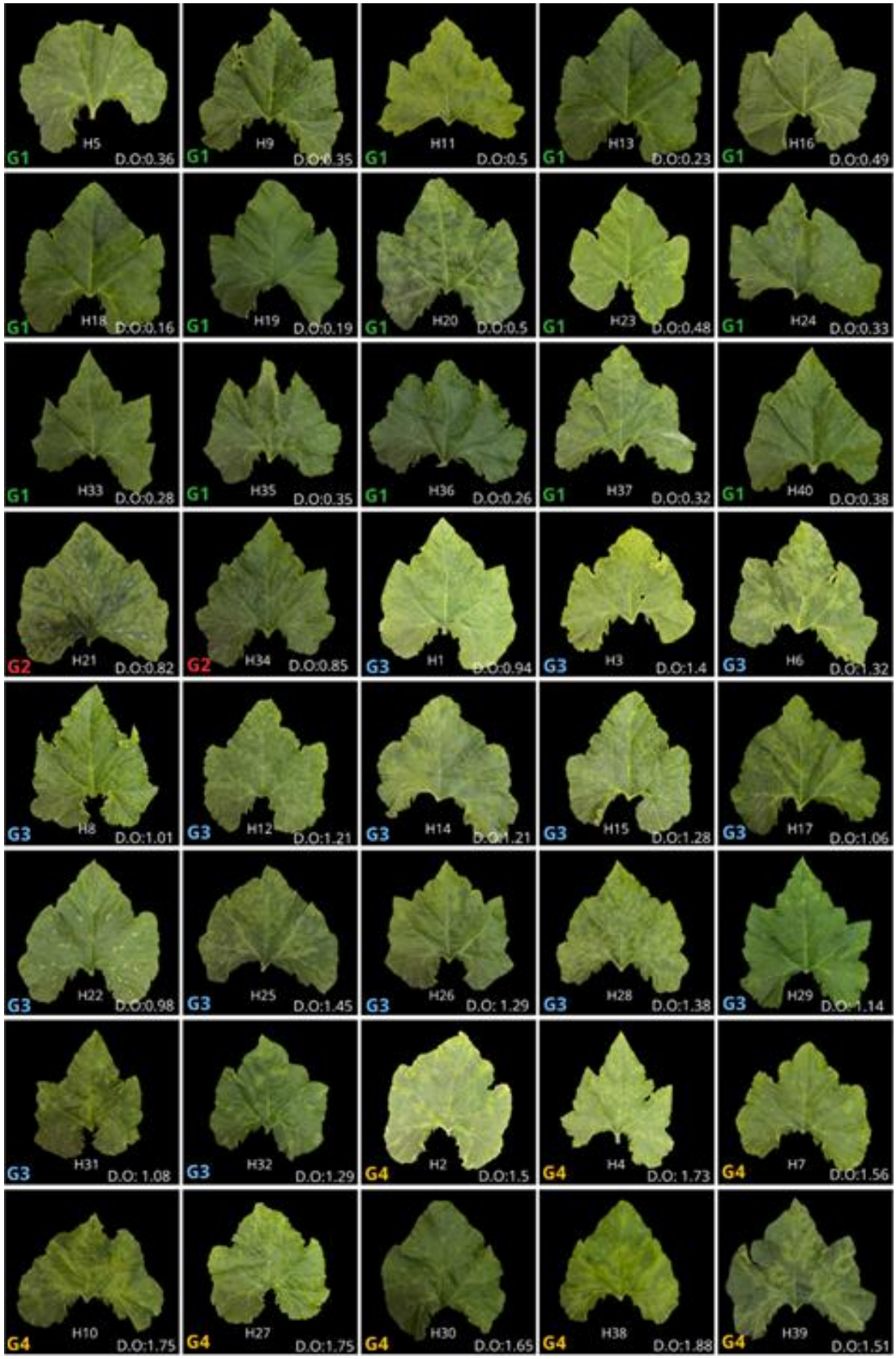


Figure 4. Images of 40 leaves of *C. moschata*, each collected from different plants, showing varying levels of viral infection severity at 217 days after transplanting. At the bottom of each image, the severity grade (G), leaf code (H), and optical density (OD) are indicated. Severity grades are represented by color: green (G1), red (G2), blue (G3), and orange (G4). OD values were obtained by DAS-ELISA.

In this context, the absorbance values obtained in the present study fall within these thresholds, supporting the accuracy of virus detection.

The threshold value (OD = 0.64) proved suitable for the conditions evaluated in this study; however, samples close to this value should be interpreted with caution. In addition, WMV and PRSV were not specifically evaluated, and their possible occurrence in mixed infections cannot be completely ruled out.

3.3. Development of an ordinal diagrammatic severity scale for ZYMV

Based on optical density (OD) values obtained from DAS-ELISA analysis of 40 leaf samples, combined with severity levels documented through photographic records, an ordinal diagrammatic scale was developed to integrate serological data with the visual expression of symptoms (Figure 5). Accordingly, a four-level ordinal severity scale was established.

Severity level 1 (Grade 1), comprised 10 samples with OD values ranging from 0.20 to 0.64, characterized by the absence of symptoms or the presence of mild mottling. Severity level 2 (Grade 2), included samples with OD values between 0.65 and 0.90, exhibiting symptoms ranging from mottling to mild mosaic patterns. Severity level 3 (Grade 4) consisted of 15 samples with OD values between 0.90 and 1.49. Leaves in this group were characterized by prominent mosaic symptoms with intense coloration, affecting approximately 50% of the leaf area. However, four samples within this level showed lower intensity and reduced damage extent. Severity level 4 (Grade 4), included eight samples with OD values greater than 1.50, characterized by severe and intense mosaic symptoms distributed across the entire leaf blade or in localized areas.

Following the analysis of groupings and the continuity of traits across severity levels, an ordinal diagrammatic scale for foliar symptoms of ZYMV in *C. moschata* was established (Figure 5). The ordinal severity scale, composed of four levels (1 – 4) and based on foliar symptomatology and optical density values, was applied across multiple evaluations by different observers on leaves exhibiting varying degrees of symptom severity.

The observed relationship between viral severity and agronomic impact suggests that tolerance should not be assessed solely based on the absence of symptoms. In this regard, Sabharwal et al. (2024) indicate that accuracy in disease assessment constitutes a key limiting factor for the success of modern breeding programs, emphasizing that, without an appropriate scale capturing severity progression, it is difficult to distinguish between mechanical resistance and physiological tolerance. The categorization of viral symptoms, ranging from mild mosaic patterns to severe deformation and foliar blistering, observed in the present study, is consistent with the methodology proposed by Elbaz et al. (2022), who highlighted that the use of numerical categories is essential for calculating severity indices and performing robust statistical comparisons among cultivars. In this context, the use of standardized assessment tools is critical for distinguishing between complete resistance, tolerance, and susceptibility, particularly given the high biological variability associated with ZYMV (Desbiez, 2020; Dhillon et al., 2021). Ordinal scales are particularly useful for viral diseases characterized by symptoms such as mosaics, deformation, and blistering, which are not easily quantified using leaf area–based methods (Shi et al., 2023).

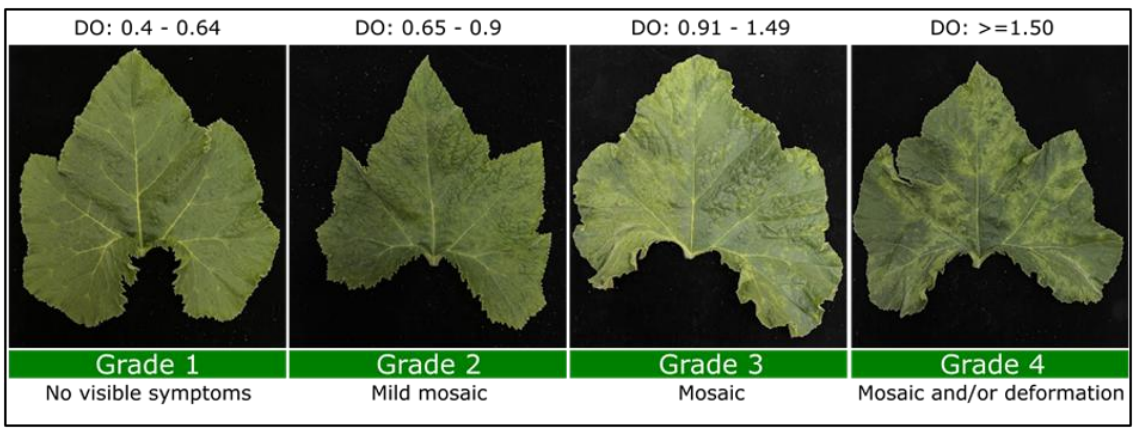


Figure 5. Ordinal diagrammatic scale for assessing ZYMV severity in *C. moschata*, illustrating the progression of symptoms from mild to severe. The upper panel shows the corresponding range of optical density (OD) values obtained from DAS-ELISA.

The integration of accurate severity scales represents a robust strategy to support the sustainability of squash production in the face of ZYMV expansion in Peru (Valencia et al., 2025). This approach enables the conversion of qualitative observations into quantifiable and analyzable data, constituting a fundamental practice for precise phenotyping in plant breeding programs. In this context, Xu et al. (2004) evaluated the inheritance of resistance to ZYMV and watermelon mosaic virus (WMV) by crossing resistant and susceptible plants, using an ordinal severity scale ranging from 0 to 5. Similarly, Wutue et al. (2025) adapted a visual scale with 0–4 levels, originally developed for the evaluation of okra mosaic virus (OMV) in okra (Ndunguru & Rajabu, 2004), and applied it across 123 cucurbit fields to assess the impact of Moroccan watermelon mosaic virus (MWMV), reaching maximum severity values of 3.8.

3.4. Validation and application of the ZYMV severity scale

3.4.1. Biological consistency of the severity scale

To validate the biological accuracy of the proposed visual scale, the correlation between the assigned ordinal severity levels and the serological absorbance (OD at 405 nm) obtained via DAS-ELISA was evaluated. Spearman's rank correlation analysis demonstrated a very strong and highly significant positive association ($\rho = 0.937$, $p < 0.0001$). This confirms that the progressive increase in visual symptomatology described in the scale accurately reflects the increase in ZYMV antigen concentration in *C. moschata* leaf tissue (Figure 6).

The strong association between viral concentration, symptom severity, and their assigned levels on our scale confirms that visual ZYMV progression in susceptible hosts is directly driven by viral multiplication, and that the severity levels of the proposed scale adequately represent this progression. This pattern aligns with findings from other viral pathosystems, such as rice black-streaked dwarf virus (RBSDV) (Han et al., 2019), groundnut bud necrosis virus (GBNV) (Gupta et al., 2021), and rice stripe necrosis virus (RSNV) (do Nascimento et al., 2024). Although DAS-ELISA is generally less sensitive than molecular techniques (e.g., RT-qPCR) at low viral concentrations, and often exhibits a reduced capacity to detect significant differences in viral load at the lowest severity levels (Wang et al., 2006; Han et al., 2019), applying a strict detection threshold and establishing a wider separation between the proposed severity levels mitigated these limitations and biologically supported the proposed categories. Nevertheless, we concur that visual assessment of resistance should serve as an initial screening tool, to be complemented with viral quantification when evaluating highly promising materials. Furthermore, this robust concentration–severity correlation must be interpreted with caution in the context of tolerance or partial resistance, where plants displaying mild symptoms may still harbor high viral titers (Jeger, 2022).

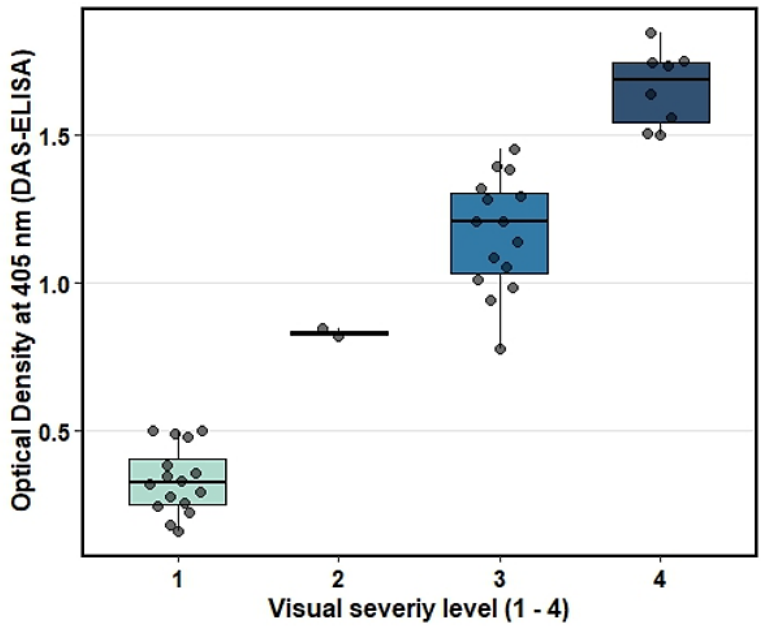


Figure 6. ZYMV samples optical density (DAS-ELISA) according to assigned visual severity levels. The strong positive association between the visual scale and viral load was confirmed by Spearman's rank correlation ($\rho = 0.937$, $p < 0.0001$). Individual observations are shown as dots overlaying the boxplots.

3.4.2. Inter-rater reliability of the severity scale

The reliability of field results obtained using the severity scale proposed in this study was assessed through inter-rater agreement analysis (Figure A3). As shown in Table 2, pairwise agreement based on Cohen's kappa was significant for all evaluator combinations and indicated strong agreement among evaluators E1, E2, and E3, with the highest agreement observed between E2 and E3 (kappa = 0.6593; $p < 0.001$). In contrast, pairings involving evaluator E4 with E1 (kappa = 0.4982; $p < 0.001$) and E2 (kappa = 0.5871; $p < 0.001$) showed moderate but still significant concordance. Overall inter-rater concordance, assessed using Fleiss' kappa, indicated a strong and significant level of agreement among all evaluators (kappa = 0.608; $p < 0.001$), with 45 out of 96 evaluated units showing complete agreement in severity level assignments across the four evaluators. When agreement was analyzed by severity level, the highest and very strong agreement was observed for severity level 1 (kappa = 0.7156; $p < 0.001$), with complete agreement among all evaluators in 14 leaves (56/84 observations). This was followed by severity level 4 (kappa = 0.6329; $p < 0.001$), which showed strong agreement, with consensus among all four evaluators in six leaves (24/59 observations). Similarly, intermediate severity levels showed significant moderate agreement ($p < 0.001$), with kappa values of 0.5945 and 0.5159 for severity levels 2 (15 leaves and 60/131 observations) and 3 (10 leaves and 40/110 observations), respectively.

Although alternative methods exist to verify the reliability of ordinal disease scales, such as those recommended by Madden et al. (2007b) and González-Concha et al. (2021) to account for sequential weighting, this study employed Cohen's and Fleiss's kappa concordance analyses. This approach conferred greater stringency to the evaluation, yielding strong and highly significant agreement across all comparisons, thereby confirming the proposed scale's high reliability.

Regarding the scale's structure, ZYMV severity scales (Table 3), like those of other viral pathosystems (Xu et al., 2004; do Nascimento et al., 2024), typically comprise five or more levels, our four-level design proved highly robust. As anticipated, the highest reliability was observed at the extreme ends of the scale, with a slight, yet acceptable, reduction at the intermediate levels. This demonstrates that the number of levels and their respective ranges, established by correlating visual severity with viral load via optical density, were optimally defined, successfully facilitating an accurate visual distinction of symptoms by raters with varying levels of experience. While ordinal scales facilitate rapid and high-throughput evaluations, their subjectivity in assigning severity levels and lack of a quantitative threshold to approximate actual disease severity remain major drawbacks in the ZYMV context (Madden et al., 2007b).

Table 3 compares disease severity scales, resistance sources or elicitors, and statistical validation criteria across cucurbit species. While previous studies have widely proposed or used visual scales for ZYMV, their biological consistency was frequently assessed only descriptively or qualitatively to confirm virus presence. Furthermore, formal phytopathometric validation has been largely absent. To address this methodological gap, the present study standardizes a 1 – 4 visual scale across two quantitative dimensions. First, biological accuracy or validity was confirmed by correlating visual grades with relative viral concentration (DAS-ELISA absorbance) using Spearman's rank correlation. Second, reproducibility was established through inter-rater reliability evaluated by overall Fleiss' and pairwise Cohen's kappa concordance analyses. This dual-validation approach provides a biologically grounded and highly reproducible phenotyping tool, laying a solid foundation for ZYMV resistance screening in *C. moschata* breeding programs.

Table 2

Concordance based on Cohen's Kappa, Fleiss' Kappa, and the proportion of observation with the same severity level according to raters [a]

Rater[b]	E2	E3	E4
E1	71/96; z = 10.757 (0.6457 ^{sig})	71/96; z = 10.631 (0.6433 ^{sig})	91/96; z = 8.200 (0.4982 ^{sig})
E2		72/96; z = 10.942 (0.6593 ^{sig})	67/96: z = 9.727 (0.5871 ^{sig})
E3			69/96; z = 10.036 (0.6124 ^{sig})
E4			
Global [c]	Kappa = 0.608 ^{sig}; z = 24.5 (p<0.001) (45/96)		

[a] Leaves were independently classified by each rater using the proposed severity scale (levels 1–4). Kappa values statistically different from zero (excluding agreement by chance) are reported in parentheses and marked with the superscript *sig*, based on the z-statistic ($p < 0.001$). Additionally, the exact agreement percentage is presented, representing the proportion of leaves assigned to the same severity level for each pair of raters.

[b] Cohen's kappa coefficient used to estimate pairwise agreement between raters.

[c] Fleiss' kappa coefficient used to determine the overall agreement among the four-rater panel.

Table 3
Comparison of disease severity scales, resistance sources or elicitors, and validation criteria for ZYMV across cucurbit species between the current study and previous literature

Assessed species (References)	Scale levels	Basis for the levels	Sources of resistance	Statistical validation*
Cucurbita moschata (Current study)	1 = no visible symptoms; 2 = mild mosaic; 3 = mosaic; 4 = mosaic and/or leaf deformation.	Ordinal scale based on foliar symptoms, biologically standardized with viral concentration.	*Cucurbita moschata* accessions C44 and C09.	Biological consistency (accuracy) between visual disease severity grades and viral concentration (DAS-ELISA absorbance, OD at 405 nm) validated by Spearman's rank correlation analysis (ρ; $\alpha = 0.05$). Inter-rater reliability of visual estimates validated via overall concordance (Fleiss' kappa) and pairwise agreement (Cohen's kappa) analyses.
Cucurbita pepo (Riquelme-Verastegui et al., 2026)	0 = no symptoms; 1 = mild mosaic; 2 = mosaic; 3 = mosaic with blistering and leaf deformation; and 4 = severe leaf reduction with deformation.	Ordinal scale based on foliar symptoms.	*Cucurbita pepo* cv. 'Rocío F1'.	Not validated.
Cucurbita pepo (Metwally et al., 2024)	0 = no symptoms; 1 = mild mosaic; 2 = mottling; 3 = mild mosaic, mottling, and blisters; 4 = severe mosaic, green blisters, and vein banding; and 5 = severe mosaic, green blisters, vein banding, and filiform.	Ordinal scale based on foliar symptoms.	Systemic resistance induced by the application of arbuscular mycorrhizal fungi (AMF).	Biological consistency between visual disease severity and viral concentration evaluated by DAS-ELISA for descriptive purposes only.
Cucurbita pepo (Ghanem et al., 2023)	0 = no symptoms; 1 = slight mottling or lightening of the veins; 2 = light mosaic; 3 = severe mosaic and blistering; 4 = leaf deformation; 5 = severe stunting of the plant.	Ordinal scale based on leaf and whole-plant symptoms.	Systemic resistance induced by applications of cultures of *Streptomyces* spp.	Biological consistency between visual disease severity and viral load (P1 gene expression quantified by RT-qPCR) analyzed via ANOVA and Duncan's multiple range test.
Cucurbita moschata (Shrestha et al., 2021)	0 = no symptoms; 1 = yellowing, mottling, and blistering of the leaves.	Binary qualitative scale based on foliar symptoms.	Genetic resistance from *C. moschata* landrace 'Nigerian Local'.	Statistical association between the visual resistance phenotype (binary scale) and specific molecular markers (SNPs) validated by the Kruskal-Wallis test.
Cucurbita pepo (Sofy et al., 2014)	0 = no symptoms; 1 = mild mosaic; 2 = mottling; 3 = mild mosaic, mottling and blisters; 4 = severe mosaic, green blisters and vein banding; and 5 = severe mosaic, green blisters, vein banding and filiform leaves.	Ordinal scale based on foliar symptoms.	Systemic resistance induced by applications of an aqueous extract of *Salix alba* and a filtrate of *Spirulina* sp.	Biological consistency between visual disease severity and viral concentration quantified by DAS-ELISA for descriptive purposes only.
Cucurbita pepo, Cucumis sativus, Citrullus lanatus, Cucurbita moschata (Svoboda et al., 2013)	Immune = no symptoms; Resistant / Moderately resistant = mild mosaic patterns or diffuse yellow spots on leaves, non-deformed fruit; Tolerant = mosaic on leaves but fruit nearly without deformation; Susceptible = systemic mosaic, dark green blisters on leaves, deformed lumpy fruit; Highly susceptible = severe leaf deformation (shoestringing), severe mosaic, severely deformed fruit, or premature plant death.	Qualitative ordinal scale based on leaf and whole-plant symptoms.	*C. sativus* cv. 'Taichung Mou Gua-1' (TMG-1); *C. lanatus* accession PI 595203; and *C. moschata* cv. 'Menina 15' and 'Nigerian Local'.	Biological consistency between descriptive phenotypic categories and relative virus concentration (DAS-ELISA), with absolute immunity validated by RT-PCR.
Citrullus lanatus (Xu et al., 2004)	0 = no symptoms; 1 = slightly mosaic on leaves; 2 = mosaic patches and/or necrotic spots on leaves; 3 = leaves near apical meristem deformed slightly, yellow, and reduced in size; 4 = apical meristem with mosaic and deformation; and 5 = extensive mosaic and serious deformation of leaves, or plant dead.	Ordinal scale based on leaf and whole-plant symptoms.	*Citrullus lanatus* accession PI 595203 (qualitative inheritance controlled by a single recessive gene, *zym-CH*).	Biological consistency between asymptomatic/resistant phenotypes (grades 0–2) and negative ELISA results for descriptive confirmation, with qualitative inheritance validated statistically by χ^2 goodness-of-fit tests.
Cucumis sativus (Park et al., 2000)	1 = no symptoms; 3 = slight mosaic limited to lower leaves; 5 = clear mosaic on lower leaves and slight mosaic on upper leaves; 7=moderate mosaic on upper leaves; 9 = severe mosaic on all leaves.	Ordinal scale based on foliar symptoms.	*C. sativus* line TMG-1/Taichung Mou Gua.	Statistical association between severity phenotypes (disease severity index) and molecular markers (AFLP, RFLP, RAPD) validated by linkage analysis (LOD ≥ 3.5) and χ^2 goodness-of-fit tests.

* Statistical validation of the reliability, reproducibility, and precision, or biological consistency, of the scale's levels (Madden et al., 20017a).

3.4.3. Differential response of *C. moschata* accessions to ZYMV

The distribution of observations according to ZYMV severity levels was not homogeneous among accessions. A highly significant association was found between accession and severity level (χ^2 = 96.076; p = 0.0004). Based on the observed data, the strength of this association was moderate, as indicated by Cramér's V (0.2873), and reached a strong level when estimated from simulated data, with a 95% confidence interval (CI) ranging from 0.304 to 0.381.

As shown in Figure 7, accession C44 exhibited a higher frequency of observations at severity level 1 than expected under independence or random distribution (standardized residual = 2.9). In contrast, a negative association was observed with the highest severity level (standardized residual = −2.29), highlighting the superior response of this genotype and its potential as the most promising against ZYMV. A similar pattern was observed for accession C25.

Conversely, accession C41 showed a significantly negative association with the lowest severity level (standardized residual = −2.27) and, despite the lack of statistical significance, displayed the strongest association with severity level 4 (standardized residual = 1.9), indicating its poorer performance in response to ZYMV.

Analysis of variance (ANOVA) performed on aligned rank transformed (ART) data revealed highly significant differences in ZYMV severity among the evaluated accessions (p < 0.001). However, no significant differences were detected for the main effect of replicate (p = 0.128). Therefore, when evaluating the main effect of accessions (Figure 8), accession C44 exhibited the lowest severity (mean score = 1.67; aligned rank = 108), differing significantly from the susceptible genotypes (p < 0.05). This was followed by accessions C09 (1.83; aligned rank = 130) and C25 (1.92; aligned rank = 142), which formed a second group of low severity and differed significantly from the most susceptible accession C41 (p < 0.05). In contrast, accession C41 presented the highest severity (2.92; aligned rank = 255), positioning it as the most susceptible genotype.

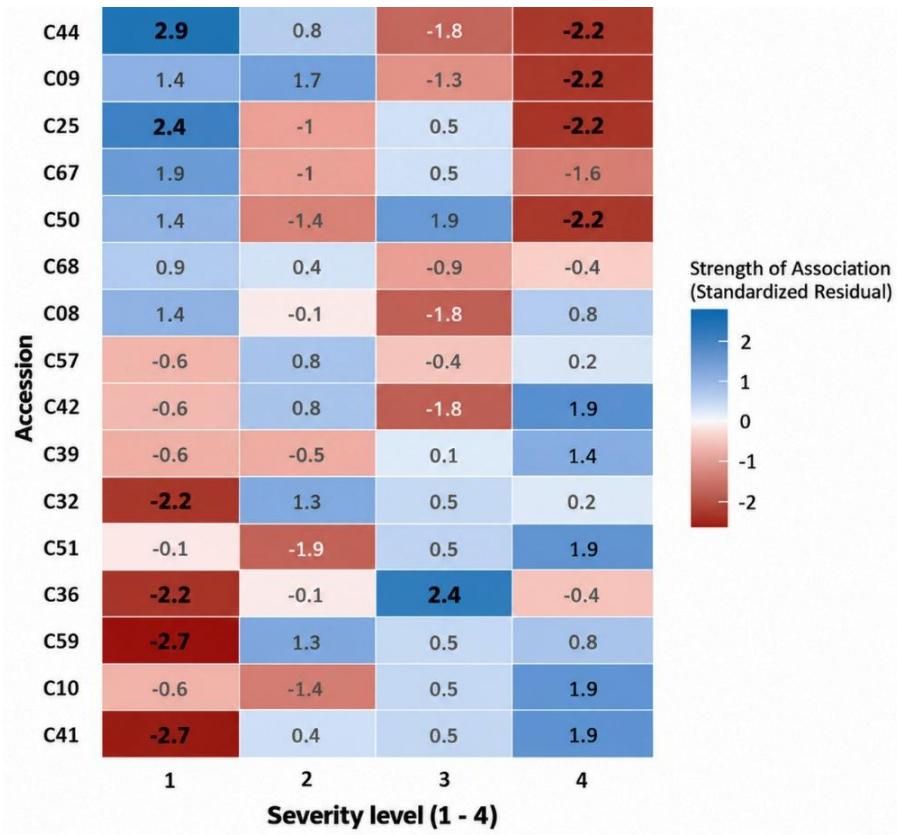


Figure 7. Heatmap of associations between accessions and ZYMV severity levels (1–4). Numeric values represent standardized residuals from the χ^2 test of independence (p = 0.0004). Significant combinations, indicating deviations from the expected frequencies under the null hypothesis of independence, are highlighted in bold. Standardized residual values > 1.96 (blue) indicate a significant positive association (observed frequency higher than expected by chance), whereas values < -1.96 (red) indicate a significant negative association (observed frequency lower than expected).

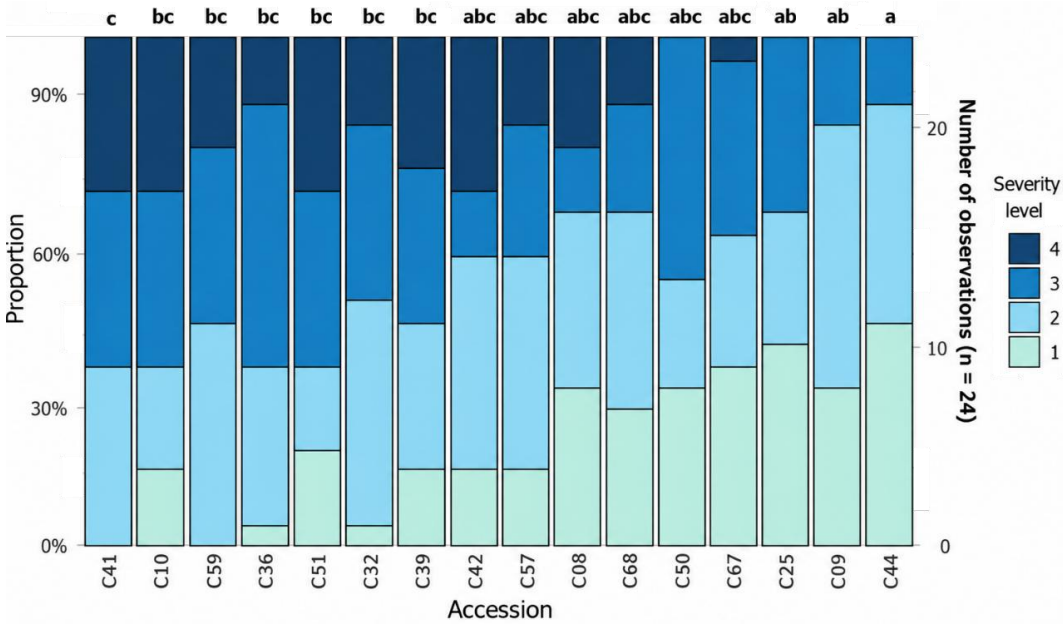


Figure 8. Frequency distribution of ZYMV severity by accession. Accessions are ordered from highest to lowest severity. Different letters in parentheses at the top indicate significant differences among accessions based on an ANOVA of ART-transformed ranks ($p < 0.001$), followed by pairwise comparisons using the t-test with Bonferroni adjustment ($p < 0.05$).

Analysis of the accession × replicate interaction ($p < 0.001$) indicated that disease severity varied spatially in only three of the sixteen accessions (Figure A4). Notably, genotype C44, which showed the lowest overall severity, exhibited a stable and consistent response across both replicates ($p = 0.375$), a pattern also observed for accessions C09 ($p = 0.349$) and C25 ($p = 0.787$). In contrast, the significant interaction was driven exclusively by accessions C67 ($p = 0.0003$), C39 ($p = 0.0061$), and C68 ($p = 0.0042$), which displayed variability in disease severity depending on the replicate in which they were established.

The absence of symptoms or the presence of attenuated symptoms may be associated with sources of tolerance that could be exploited in the Vegetable Research Program at UNALM. Accessions C44 and C09 exhibited the highest frequencies at the lowest severity levels among the sixteen evaluated accessions, highlighting their potential as promising material for future resistance studies. These findings are consistent with previous reports demonstrating the existence of resistance genes to potyviruses in *C. moschata*. In the Portuguese cv. 'Menina', the dominant gene *Zym* was identified, conferring resistance to ZYMV and WMV-2 (Paris et al., 1988; Gilbert-Albertini et al., 1993). Likewise, the genes *Wmv* and *Cmv*, associated with monogenic resistance to WMV and CMV, respectively, as well as the recessive gene *prv*, conferring resistance to PRSV, have been described (Brown et al., 2003).

In addition, segregation studies have identified loci *Zym-0*, *Zym-1*, *Zym-4*, *zym-5*, and *zym-6*, highlighting the interaction between *Zym-4* and *zym-5* for resistance expression, as well as the potential linkage of *zym-6* and *Zym-1* with other resistance loci (Pachner et al., 2011). More recently, Shrestha et al. (2022) identified in *C. moschata* a QTL associated with resistance to PRSV-W on chromosome 9, validated using KASP markers linked to defense-related genes.

Collectively, these findings support the hypothesis that the differential response observed among accessions has a genetic basis, reinforcing the relevance of C44 and C09 as potential sources of resistance for breeding programs aimed at managing ZYMV. The identification of accessions with lower severity, such as C44 and C09, opens new opportunities for their incorporation into breeding programs through intra- or interspecific crosses in cucurbits, contributing to the sustainable management of this virus.

4. Conclusions

In this study, a four-level ordinal diagrammatic scale was developed and rigorously validated to assess and quantify ZYMV severity in *Cucurbita moschata*. By demonstrating both biological accuracy and high inter-rater reliability, with biological accuracy supported by serological quantification, the scale emerged as a highly consistent and reproducible tool.

Under field conditions, its application enabled the effective evaluation of disease progression across sixteen accessions, successfully identifying C44, followed by C09, as the genotypes exhibiting the highest resistance to the virus. The implementation of such exact and standardized assessment tools facilitates the reliable screening and selection of promising genetic materials in plant breeding programs aimed at viral resistance. Notably, C44 and C09 exhibited the lowest mean severity scores (levels 1–2), with significant differences ($p < 0.05$), indicating their potential as resistant genotypes.

Further validation of the scale across different locations and growing seasons is recommended to support its broader application in breeding programs.

Author contributions

FGB: investigation, methodology, data curation, writing – original draft. **DMG:** conceptualization, methodology, data curation, formal analysis, validation, writing – original draft, writing – review & editing. **IMY:** resources, validation, supervision, writing – review & editing. **ADD:** conceptualization, funding acquisition, writing – review & editing. **ARM:** conceptualization, methodology, project administration, supervision, writing – review & editing.

Acknowledgments

The authors acknowledge the financial support provided by the Vegetable Research and Social Outreach Program and the Virology Area of the Department of Plant Pathology, Faculty of Agronomy, Universidad Nacional Agraria La Molina, which made this research possible.

Conflict of interest

The authors declare no conflicts of interest.

ORCID

F. Gonzales Borda https://orcid.org/0009-0005-0114-6583

D. Marin-Gil https://orcid.org/0000-0003-0163-5887

I. M. Montes-Yarasca https://orcid.org/0000-0002-1285-8413

A. Dueñas https://orcid.org/0000-0002-6149-3334

A. Risco-Mendoza https://orcid.org/0000-0001-9890-9404

References

Ahsan, M., Ashfaq, M., Amer, M. A., Shakeel, M. T., Mehmood, M. A., Umar, M., & Al-Saleh, M. A. (2023). Zucchini yellow mosaic virus (ZYMV) as a serious biotic stress to cucurbits: Prevalence, diversity, and its implications for crop sustainability. *Plants*, *12*(19), 3503. https://doi.org/10.3390/plants12193503

Abdel Aleem, E. E., Rabie, M., & Fattouh, F. A. (2021). Molecular characterisation of zucchini yellow mosaic virus infecting *Cucurbita pepo* in Egypt. *Plant Protection Science*, 57(4), 263–270. https://doi.org/10.17221/191/2020-PPS

Ali, R., Eldidamony, G., Askora, A., & Galal, A. (2024). Investigates the ability of plant extracts from *Lens culinaris* to protect zucchini from the Zucchini yellow mosaic virus (ZYMV). *Scientific Reports*, *14*(1), 12257. https://doi.org/10.1038/s41598-024-62128-6

Arbizu, C. I., Blas, R. H., & Ugás, R. (2022). Genetic diversity and population structure assessed by SSR in a Peruvian germplasm collection of loche squash (*Cucurbita moschata*, Cucurbitaceae). *Biology and Life Sciences Forum*, *6*, 20. https://doi.org/10.3390/iecd2022-12420

Blua, M. J., & Perring, T. M. (1989). Effect of zucchini yellow mosaic virus on development and yield of cantaloupe (*Cucumis melo*). *Plant Disease*, 73(4), 317-320. https://doi.org/10.1094/PD-73-0317

Bock, C. H., Chiang, K. S., & Del Ponte, E. M. (2022). Plant disease severity estimated visually: A century of research, best practices, and opportunities for improving methods and practices to maximize accuracy. *Tropical Plant Pathology*, *47*, 25–42. https://doi.org/10.1007/s40858-021-00439-z

Boissinot, S., Pichon, E., Sorin, C., Piccini, C., Scheidecker, D., Ziegler-Graff, V., & Brault, V. (2017). Systemic propagation of a fluorescent infectious clone of a polerovirus following inoculation by Agrobacteria and aphids. *Viruses, 9*(7), 166. https://doi.org/10.3390/v9070166

Brown, R. N., Bolaños-Herrera, A., Myers, J. R., & Miller Jahn M. (2003). Inheritance of resistance to four cucurbit viruses in *Cucurbita moschata*. *Euphytica, 129(3)*, 253–258. https://doi.org/10.1023/A:1022224327064

Caligiore-Gei, P. F., Della-Gaspera, P., Benitez, E., & Tarnowski, C. (2022). Cucurbit Powdery Mildew: First Insights for the Identification of the Causal Agent and Screening for Resistance of Squash Genotypes (*Cucurbita moschata* (Duchesne ex Lam.) Duchesne ex Poir.) in Mendoza, Argentina. *The Plant Pathology Journal*, 38(4), 296. https://doi.org/10.5423/ppj.oa.01.2022.0002

Candian, J. S., Coolong, T., Dutta, B., Srinivasan, R., Sparks, A., Barman, A., & Ribeiro, A. (2021). Selection of yellow squash and zucchini cultivars for resistance to cucurbit leaf crumple virus in the southeastern United States. *HortTechnology, 31*(4), 504–513. https://doi.org/10.21273/HORTTECH04877-21

Chen, T. C., Kang, Y. C., Tran, T. N. B., Huang, L. H., Lin, C. C., & Yeh, S. D. (2026). Generation of a Bivalent Recombinant Vaccine Conferring Dual Protection Against Potyvirus and Orthotospovirus in Cucurbits. *Viruses*, 18(2), 250. https://doi.org/10.3390/v18020250

Desbiez, C. (2020). The never-ending story of cucurbits and viruses. *Acta Horticulturae, 1294*, 173–191. https://doi.org/10.17660/ActaHortic.2020.1294.23

de la Iglesia, F., & Elena, S. F. (2023). Effect of disease prevalence and growth stage on symptom severity in the Turnip mosaic virus–*Arabidopsis thaliana* pathosystem. *Journal of Plant Protection Research*, 63(3), 297–305. https://doi.org/10.24425/jppr.2023.145762

Dhillon, N. P. S., Srimat, S., Laenoi, S., Bhunchoth, A., Phuangrat, B., Warin, N., & Kenyon, L. (2021). Resistance to three distinct begomovirus species in the agronomical superior tropical pumpkin line AVPU1426 developed at the World Vegetable Center. *Agronomy, 11*(6), 1256. https://doi.org/10.3390/agronomy11061256

Díaz, A., Quiñones, M., Arana, F., Soto, M., & Hernández, A. (2010). Potyvirus: Características generales, diagnóstico y presencia en pimiento en Cuba. *Protección Vegetal*, *25*(2), 69–79.

Do Nascimento, S. C., Scheuermann, K. K., Pereira, F. S., Gorayeb, E. S., Albuquerque, M. R. M., Mendes, G. C., de Mello, R. N., Lau, D., & da Silva, F. N. (2024). Development of a severity scale and an RT-qPCR assay for screening resistance levels in rice genotypes against rice stripe necrosis virus and its vector. *Plant Pathology, 73*, 2101–2111. https://doi.org/10.1111/ppa.13952

Elbaz, M., Timoumi, M., & Hanson, P. (2022). Behavior of new entries and developed tomato hybrids carrying Ty-2 genes. *Tunisian Journal of Plant Protection, 17*(1), 1–14. https://doi.org/10.52543/tjpp.17.1.1

Fidan, H., Calis, O., Ari, E., Atasayar, A., Sarikaya, P., Tek, M. I., Izmirli, A., Oz, Y., & Firat, G. (2023). Knockout of eIF4E using CRISPR/Cas9 for large-scale production of resistant cucumber cultivar against WMV, ZYMV, and PRSV. *Frontiers in Plant Science, 14*, 1143813. https://doi.org/10.3389/fpls.2023.1143813

Gea-Caballero, E., & Aranda, M. A. (2026). Cucumber green mottle mosaic virus: A persistent seed-borne threat to cucurbits. *Annals of Applied Biology*, 189(1). https://doi.org/10.1111/aab.70136

Ghanem, G. A. M., Mahmoud, A. M. A., Kheder, A. A., Gebily, D. A., & Osamy, A. (2023). Antiviral activities of three Streptomyces spp. against Zucchini yellow mosaic virus (ZYMV) infecting squash (*Cucurbita pepo* L.) plants. *Egyptian Journal of Biological Pest Control*, 33(1). https://doi.org/10.1186/s41938-023-00750-8

Ghoshal, C., Das, K., Mandal, S., & Kumar, S. (2026). Host Plant Resistance to Important Viruses in Cucurbits- Current Challenges and Advances. *Microbiology Research Journal International*, 36(2), 1–24. https://doi.org/10.9734/mrji/2026/v36i21703

Gilbert-Albertini, F., Lecoq, H., Pitrat, M., et al. (1993). Resistance of *Cucurbita moschata* to watermelon mosaic virus type 2 and its genetic relationship to resistance to zucchini yellow mosaic virus. *Euphytica*, *69*, 231–237. https://doi.org/10.1007/BF00022369

González-Concha, L. F., Ramírez-Gil, J. G., García-Estrada, R. S., Rebollar-Alviter, Á., & Tovar-Pedraza, J. M. (2021). Spatiotemporal analyses of tomato brown rugose fruit virus in commercial tomato greenhouses. *Agronomy*, 11(7), 1268. https://doi.org/10.3390/agronomy11071268

Gupta, D., Singh, O. W., Basavaraj, Y. B., Roy, A., Mukherjee, S. K., & Mandal, B. (2021). Direct Foliar Application of dsRNA Derived From the Full-Length Gene of NSs of Groundnut Bud Necrosis Virus Limits Virus Accumulation and Symptom Expression. *Frontiers in Plant Science*, 12, 734618. https://doi.org/10.3389/fpls.2021.734618

Han, X., Chen, T., Yue, R., Guo, S., Xu, M., Lu, C., Fan, Y., Chen, N., Liu, L., Fu, X., Chi, H., Guo, X., Xia, Y., & Tie, S. (2019). A rice black-streaked dwarf virus replication curve model to evaluate maize rough dwarf disease resistance. *Plant Disease*, *103*(5), 868–873. https://doi.org/10.1094/PDIS-09-18-1532-RE

Hao, X., Liu, F., Liu, L., et al. (2024). Zucchini yellow mosaic virus-induced hypersensitive response is associated with pathogenesis-related protein 1 expression and confers resistance in watermelon. *Plant Cell Reports*, *43*, 277. https://doi.org/10.1007/s00299-024-03364-y

Ibiza, V. P., Cañizares, J., & Nuez, F. (2010). EcoTILLING in *Capsicum* species: Searching for new virus resistances. *BMC Genomics*, *11*, 631. https://doi.org/10.1186/1471-2164-11-631

Jeger, M. J. (2022). Tolerancia a las enfermedades virales de las plantas: su significado genético, fisiológico y epidemiológico. *Food and Energy Security*, *12*, e440. https://doi.org/10.1002/fes3.440

Kheder, A., Sulaiman, T., Ghanem, G., & Tohamy, M. (2017). Biological, Serological and Molecular Characterization of Egyptian Zucchini Yellow Mosaic Virus Isolate Infecting Squash Plants in Fayoum Governorate. *Egyptian Journal of Phytopathology*, 45(2), 1–14. https://doi.org/10.21608/ejp.2017.88570

Lecoq, H., & Desbiez, C. (2008). Watermelon mosaic virus and zucchini yellow mosaic virus. In B. W. J. Mahy & M. H. V. Van Regenmortel (Eds.), Encyclopedia of virology (3rd ed., pp. 468-474). Academic Press. https://doi.org/10.1016/B978-012374410-4.00740-8

Li, M., Qiu, Y., Zhu, D., Xu, X., Tian, S., Wang, J., Yu, Y., Ren, Y., Gong, G., Zhang, H., Xu, Y., & Zhang, J. (2024). Editing eIF4E in the watermelon genome using CRISPR/Cas9 technology confers resistance to ZYMV. *International Journal of Molecular Sciences*, *25*(21), 11468. https://doi.org/10.3390/ijms252111468

Madden, L. V., Paul, P. A., & Lipps, P. E. (2007a). Consideration of nonparametric approaches for assessing genotype-by-environment (G × E) interaction with disease severity data. *Plant Disease*, *91*, 891–900. https://doi.org/10.1094/PDIS-91-7-0891

Madden, L. V., Hughes, G., & van den Bosch, F. (2007b). *The study of plant disease epidemics*. APS Press. https://doi.org/10.1094/9780890545058

Mahmoud, S. Y., Zia, A., Farrag, E. S., et al. (2025). Characterization of two distinct isolates of zucchini yellow mosaic potyvirus and their differential effects on photochemistry and photoprotection of the host plant. *European Journal of Plant Pathology*. https://doi.org/10.1007/s10658-025-03161-7

Metwally, R. A., Taha, M. A., Abd El-Moaty, N. M., & Abdelhameed, R. E. (2024). Attenuation of Zucchini mosaic virus disease in cucumber plants by mycorrhizal symbiosis. Plant Cell Reports, 43, Article 54. https://doi.org/10.1007/s00299-023-03138-y

Moura, M., Zerbini, F., Silva, D., & Queiroz, M. (2005). Reaction of *Cucurbita* accessions to zucchini yellow mosaic virus. *Horticultura Brasileira*, *23*(2), 206–210. https://doi.org/10.1590/S0102-05362005000200009

Navasca, A., Castleberry, C., Benz, B. R., & Baldwin, T. (2025). Quantitative assessment of *Fusarium graminearum* infection in resistant and susceptible barley genotypes beyond visual symptoms. *Phytopathology*. Advance online publication. https://doi.org/10.1094/PHYTO-07-25-0254-R

Ndunguru, J., & Rajabu, A. C. (2004). Effect of okra mosaic virus disease on the above-ground morphological yield components of okra in Tanzania. *Scientia Horticulturae*, 99(3–4), 225–235. https://doi.org/10.1016/S0304-4238(03)00108-0

Nutter, F. W., Jr., Teng, P. S., & Shokes, F. M. (1991). Disease assessment terms and concepts. *Plant Disease*, 75(11), 1187–1188. https://doi.org/10.1094/pd-75-1187

Pachner, M., Paris, H. S., & Lelley, T. (2011). Genes for resistance to zucchini yellow mosaic in tropical pumpkin. *Journal of Heredity*, 102(3), 330–335. https://doi.org/10.1093/jhered/esr006

Paris, H. S., Cohen, S., Burger, Y., et al. (1988). Monogenic resistance to zucchini yellow mosaic virus in *Cucurbita moschata*. *Euphytica*, *37*, 27–29. https://doi.org/10.1007/BF00037219

Park, Y. H., Sensoy, S., Wye, C., Antonise, R., Peleman, J., & Havey, M. J. (2000). A genetic map of cucumber composed of RAPDs, RFLPs, AFLPs, and loci conditioning resistance to papaya ringspot and zucchini yellow mosaic viruses. Genome, 43(6), 1003–1010. https://doi.org/10.1139/g00-075

Riquelme-Verastegui, P. R., Montes-Yarasca, I. M., Galvez-Gargurevich, M., French-Monar, R., & Risco-Mendoza, A. (2026). Molecular and biological characterization of Peruvian isolates of zucchini yellow mosaic virus reveals differential severity and partial resistance breakdown in zucchini cultivars. *Brazilian Journal of Biology*, 86. https://doi.org/10.1590/1519-6984.308794

Sabharwal, P., Thakur, S., Shrestha, S., Fu, Y., & Meru, G. (2024). Breeding and genetics of resistance to major diseases in *Cucurbita*: A review. *Crop Science*. https://doi.org/10.1002/csc2.21358

Saldaña Serrano, C. L., Estrada Cañari, R., Suca, E., Cruz Grimaldo, C. L., Vilcara, E., & Arbizu Berrocal, C. I. (2024). Complete chloroplast genome of a Peruvian landrace of *Cucurbita moschata*, loche, and its comparative analysis with other relative species [Preprint]. *Research Square*. https://doi.org/10.21203/rs.3.rs-5034257/v1

Schafleitner, R., Chen-yu, L., Laenoi, S., Shu-mei, H., Srimat, S., Gi-An, L., … Dhillon, N. P. S. (2024). Molecular markers associated with resistance to squash leaf curl China virus and tomato leaf curl New Delhi virus in tropical pumpkin (*Cucurbita moschata* Duchesne ex Poir.) breeding line AVPU1426. *Scientific Reports*, 14(1). https://doi.org/10.1038/s41598-024-57348-9

Shah, D. A., & Madden, L. V. (2004). Nonparametric analysis of ordinal data in designed factorial experiments. *Phytopathology*, *94*(1), 33–43. https://doi.org/10.1094/PHYTO.2004.94.1.33

Shafie, R. M., kheder, A. A., Abou-Attia, M. A., Mahmoud, N. A., Saied, S. M., Mazyad, A. A., & Abdelkader, H. S. (2026). Molecular and enzymatic insights into biocontrol-mediated

resistance against Zucchini yellow mosaic virus in squash (*Cucurbita pepo* L.). *BMC Microbiology*, 26(1). https://doi.org/10.1186/s12866-026-05161-x

Shi, T., Liu, Y., Zheng, X., Hu, K., Huang, H., Liu, H., & Huang, H. (2023). Recent advances in plant disease severity assessment using convolutional neural networks. *Scientific Reports*, 13(1), 2916. https://doi.org/10.1038/s41598-023-29230-7

Shrestha, S., Michael, V. N., Fu, Y., & Meru, G. (2021). Genetic loci associated with resistance to zucchini yellow mosaic virus in squash. *Plants*, *10*(9), 1935. https://doi.org/10.3390/plants10091935

Shrestha, S., Fu, Y., Michael, V. N., & Meru, G. (2022). Whole genome re-sequencing and bulk segregant analysis reveals chromosomal location for papaya ringspot virus W resistance in squash. *Frontiers in Plant Science*, *13*, 848631. https://doi.org/10.3389/fpls.2022.848631

Silva, G. T. M. de A., Lima, J. A. de A., Barbosa, G. da S., Souza, Ê. G. F., Oliveira, G. B. S., Queiróz, M. A. de, Silveira, L. M. da, Nascimento, A. K. Q. do, & Júnior, A. P. B. (2019). Selection of watermelon accessions for resistance to some important potyvirus species based on serological evaluation. *Australian Journal of Crop Science*, 1409. https://doi.org/10.21475/ajcs.19.13.09.p1203

Simmons, H. E., Holmes, E. C., & Stephenson, A. G. (2011). Rapid turnover of intra-host genetic diversity in zucchini yellow mosaic virus. *Virus Research*, *155*(2), 389–396. https://doi.org/10.1016/j.virusres.2010.11.011

Sofy, M. R., Sharaf, A. E. M. A., Noufl, M., & Sofy, A. R. (2014). Physiological and biochemical responses in Cucurbita pepo leaves associated with some elicitors-induced systemic resistance against zucchini yellow mosaic virus. International Journal of Modern Botany, 4(2), 61–74. https://doi.org/10.5923/j.ijmb.20140402.04

Svoboda, J., Leisova-Svobodova, L., & Amano, M. (2013). Evaluation of selected cucurbitaceous vegetables for resistance to zucchini yellow mosaic virus. Plant Disease, 97(10), 1316–1321. https://doi.org/10.1094/PDIS-11-12-1009-RE

Turechek, W. W. (2004). Nonparametric tests in plant disease epidemiology: Characterizing disease associations. *Phytopathology*, *94*(9), 1018–1021. https://doi.org/10.1094/PHYTO.2004.94.9.1018

Valencia, R., Montes, I., Dueñas, A., Blawid, R., & Risco, A. (2025). First report of zucchini yellow mosaic virus (ZYMV) infecting *Cucurbita maxima* in Peru. *Plant Disease, 109(12), 2616*. https://doi.org/10.1094/PDIS-01-25-0127-PDN

Wang, F., Qin, G., Sui, Z., Wang, Z., Wang, Z., Yu, J., & Zhang, J. (2006). Improved method for assaying maize plant resistance to maize rough dwarf disease by artificial inoculation and real-time RT-PCR. European Journal of Plant Pathology, 116(4), 289–300. https://doi.org/10.1007/s10658-006-9060-1

Wobbrock, J. O., Findlater, L., Gergle, D., & Higgins, J. J. (2011). The aligned rank transform for nonparametric factorial analyses using only ANOVA procedures. In Proceedings of the SIGCHI Conference on Human Factors in Computing Systems (pp. 143–146). Association for Computing Machinery. https://doi.org/10.1145/1978942.1978963

Wutue, A. S., Mumo, N. N., Maithya, J. K., & Ateka, E. M. (2025). Severity, incidence and distribution of Moroccan watermelon mosaic virus infecting cucurbits in selected counties in Kenya. *African Journal of Microbiology Research*, *19*(10), 236–242. https://doi.org/10.5897/AJMR2025.9814

Xu, Y., Kang, D., Shi, Z., Shen, H., & Wehner, T. (2004). Inheritance of resistance to zucchini yellow mosaic virus and watermelon mosaic virus in watermelon. *Journal of Heredity*, *95*(6), 498–502. https://doi.org/10.1093/jhered/esh076

Appendix

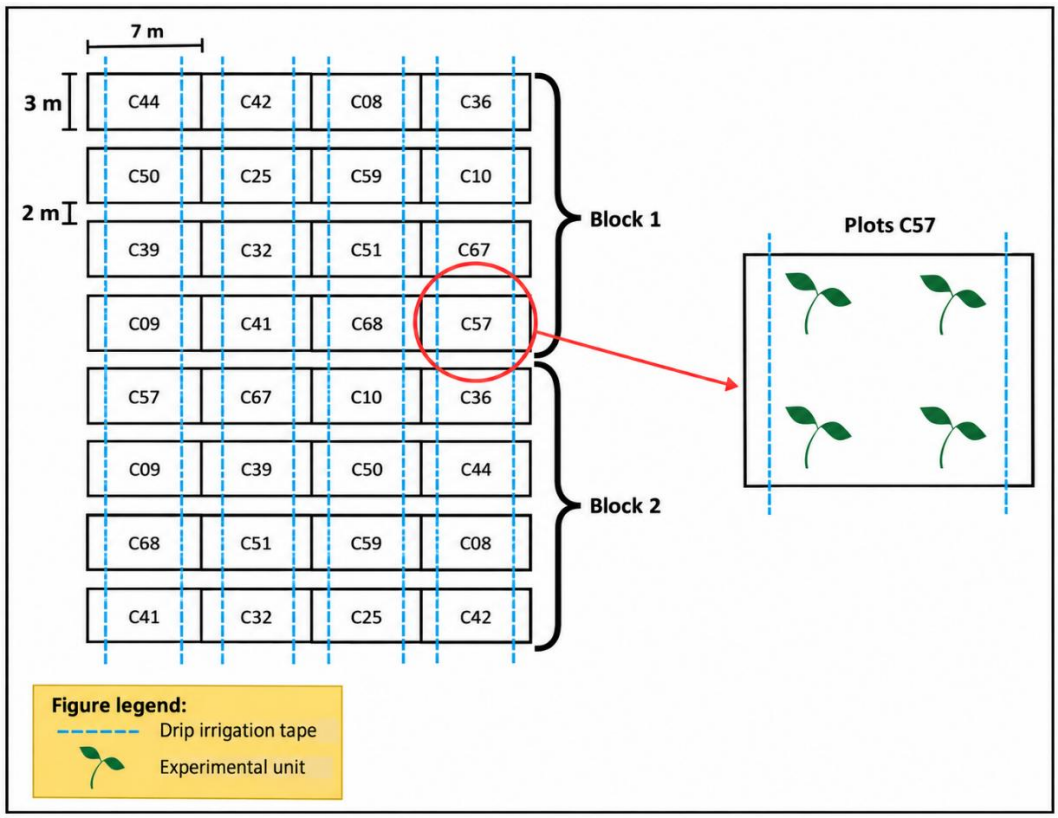


Figure A1. Schematic layout of the random distribution of the sixteen *C. moschata* accessions in the field.



Figure A2. Representative results of DAS-ELISA analysis of *C. moschata* leaf tissue for ZYMV detection.

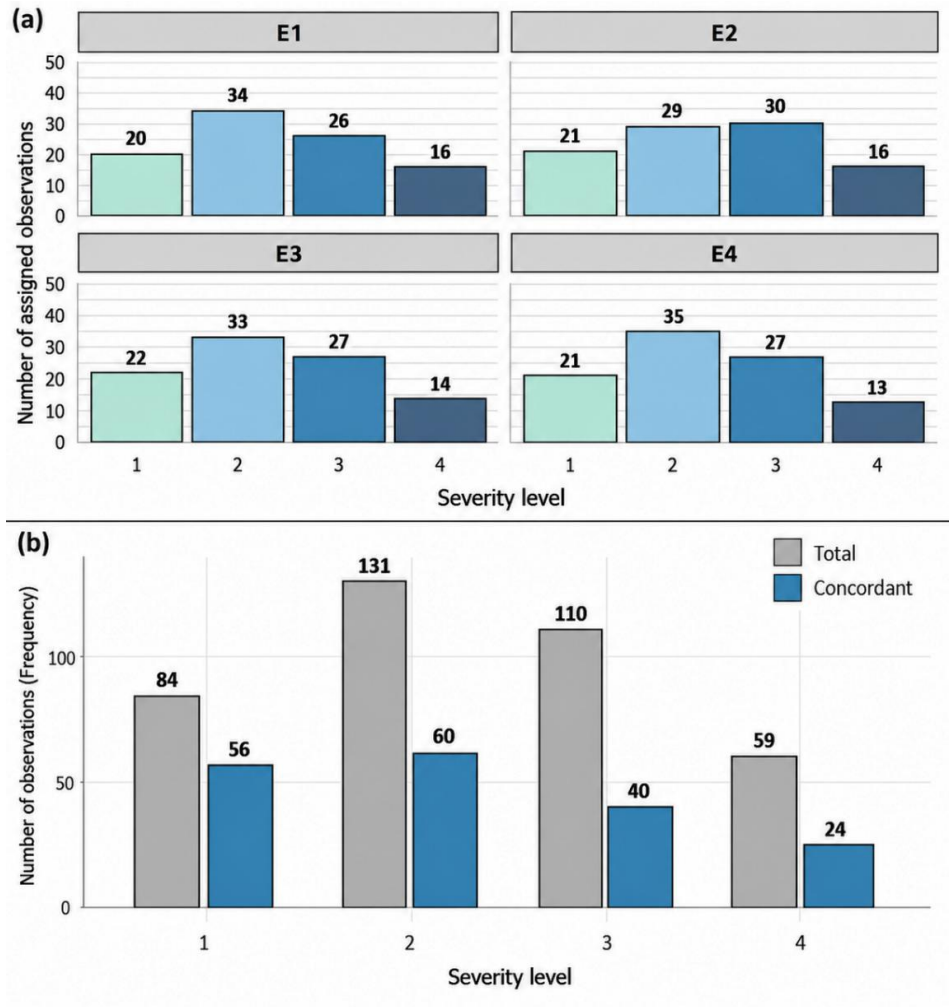


Figure A3. Frequency distribution of disease severity according to the levels of the proposed scale: (a) by evaluator; and (b) by total and concordant observations, where the gray bars represent the total number of observations per severity level, while the blue bars indicate the number of observations with complete agreement between evaluators at each level.

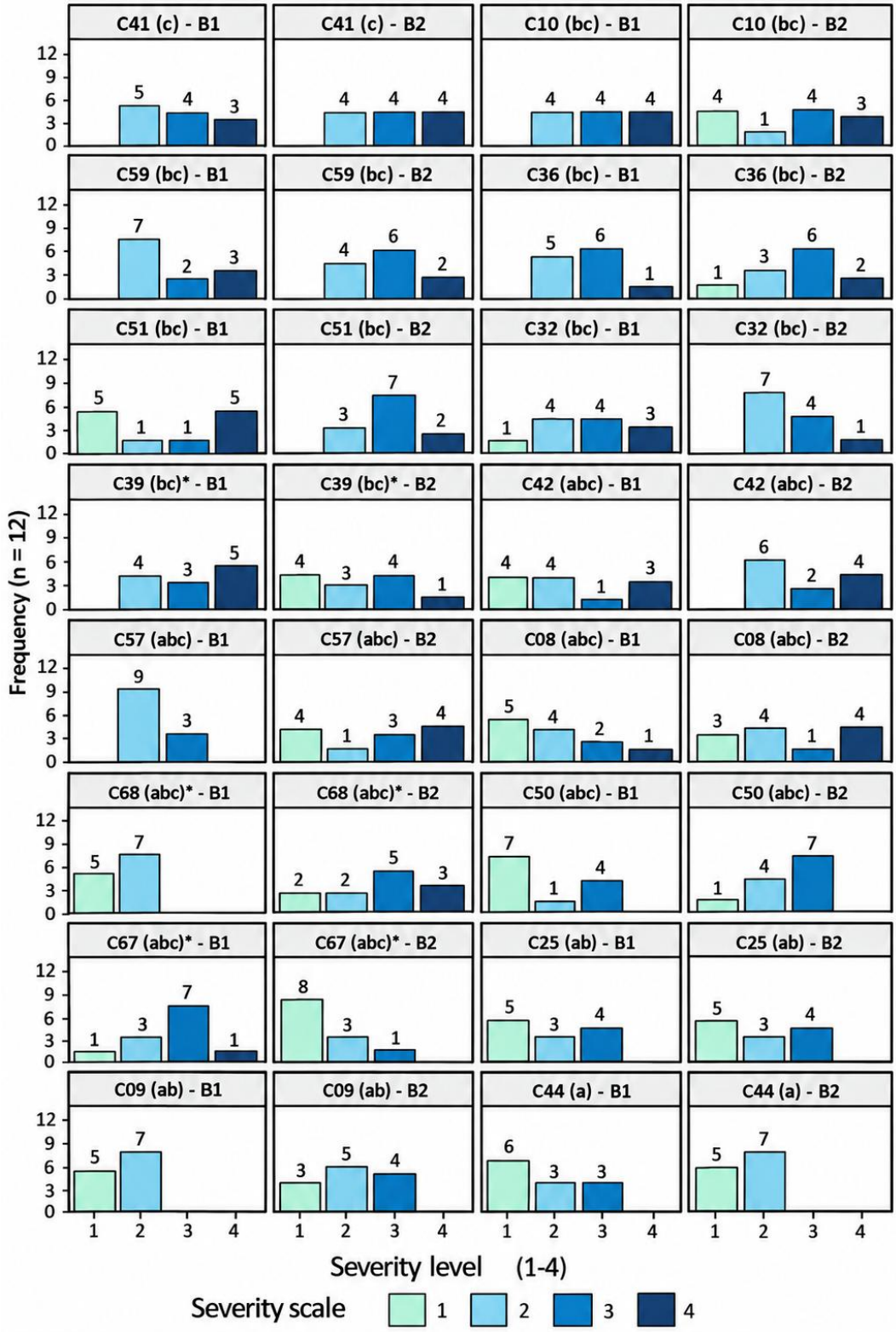


Figure A4. Frequency distribution of ZYMV severity by accession and replicate. Results are presented by accession, ordered from highest to lowest severity within each accession. Letters in parentheses indicate significant differences among accessions based on ANOVA of aligned rank transformed (ART) data ($p < 0.001$), followed by pairwise comparisons using t-tests with Bonferroni-adjusted significance ($p < 0.05$). Accessions marked with asterisks (*) indicate a significant interaction with the replicate, as determined by t-tests with Bonferroni adjustment ($p < 0.05$).